Available online at www.sciencedirect.com
ScienceDirect
Cement and Concrete Research 37 (2007) 1531–1543
Cement and Concrete Research

Supplementary cementitious materials for mitigating degradation of kraft pulp fiber-cement composites

B.J. Mohr [a,*], J.J. Biernacki [b], K.E. Kurtis [c]

[a] Department of Civil and Environmental Engineering, Tennessee Technological University, 1020 Stadium Drive, Box 5015, Cookeville, TN 38505-0001, USA
[b] Department of Chemical Engineering, Tennessee Technological University, 1020 Stadium Drive, Box 5013, Cookeville, TN 38505-0001, USA
[c] School of Civil and Environmental Engineering, Georgia Institute of Technology, 790 Atlantic Drive, Atlanta, GA 30332-0355, USA

Received 24 May 2006; accepted 2 August 2007

Abstract

Kraft pulp fiber reinforced cement-based materials are being increasingly used where performance after exposure to environmental conditions must be ensured. However, significant losses in mechanical performance due to wet/dry cycling have been observed in these composites, when portland cement is the only cementitious material used in the matrix. In this research program, the effects of partial portland cement replacement with various supplementary cementitious materials were investigated. Binary, ternary, and quaternary blends of silica fume, slag, Class C fly ash, Class F fly ash, metakaolin, and diatomaceous earth/volcanic ash blends were examined for their effect on the degradation of kraft pulp fiber-cement composite mechanical properties (i.e., strength and toughness) during wet/dry cycling. After 25 wet/dry cycles, it was shown that binary composites containing 90% slag, 30% metakaolin, or greater than 30% silica fume did not exhibit any signs of degradation, as measured through mechanical testing and microscopy. Ternary blends containing 70% slag/10% metakaolin or 70% slag/10% silica fume were also effective in preventing degradation. A reduction in calcium hydroxide content and the stability of the alkali content due to supplementary cementitious material addition were shown to be primary mechanisms for improved durability.
Published by Elsevier Ltd.

Keywords: Fiber reinforcement (E); Degradation (C); Supplementary cementitious materials; EDX (B); SEM (B)

1. Introduction

Pulp-fiber cement composites have been increasingly used as non-structural exterior building components where performance must be ensured after environmental exposure. However, it is understood that such composites may exhibit significant degradation of mechanical properties (i.e., strength and toughness) when subjected to cycles of wetting and drying [1–7]. Thus, the influence of environmental exposure on the long-term performance of pulp fiber-cement composites warrants further investigation so that appropriate mitigation strategies may be developed.

With wet/dry cycling, pulp fibers become embrittled due to the formation of cement hydration products within the fiber lumen, the fiber cell wall, and/or around the fiber [7–10]. According to a model proposed by Mohr et al. [7,10], degradation during wet/dry cycling occurs progressively by: (1) initial fiber-cement debonding, (2) reprecipitation of secondary ettringite within the void space at the former fiber-cement interface (kraft fibers only), and (3) fiber embrittlement due to reprecipitation of calcium hydroxide within the fiber lumen and/or fiber cell wall. This model, with some modifications, is also applicable to thermomechanical pulp (TMP) fiber-cement composites [6,10].

Two avenues may be explored for mitigation of fiber-cement composite degradation: (1) fiber modifications and (2) matrix modifications. Modification of the fibers, including fiber impregnation [1], fiber treatments [11], and fiber fibrillation [7,12], have been examined as means to minimize fiber-cement debonding and/or moisture migration around and through the fibers during wetting and drying. In addition, modifications affecting fiber chemical composition, dimensional stability, and fiber-cement bond strength have also been evaluated [6,7].

* Corresponding author. Tel.: +1 931 372 3546; fax: +1 931 372 6239.
E-mail address: bmohr@tntech.edu (B.J. Mohr).

0008-8846/$ - see front matter. Published by Elsevier Ltd.
doi:10.1016/j.cemconres.2007.08.001

Increases in the pulp fiber lignin content appear to improve composite durability by enhancing fiber dimensional stability, while kraft pulp drying history and fibrillation had negligible effects [6,7].

With regard to matrix modifications, the use of high alumina cement [1], matrix sealants [13], and supplementary cementitious materials (SCMs) as a partial replacement for portland cement have shown some promise. For example, silica fume, used in relatively large amounts (i.e., 30% or greater replacement of cement by weight) appears to significantly minimize composite degradation due to wet/dry cycling [1,5,14]. However, the use of slag at 40% by weight cement replacement was not found to significantly improve sisal fiber mortar composite durability after 46 wet/dry cycles [5]. Gram [1] also found no improvements in durability of sisal fiber mortar composites (after 120 wet/dry cycles) when slag was used at 70% by weight of cement replacement. Examining rice-husk ash, Ziraba et al. [11] concluded that 45% cement replacement minimized sisal fiber-mortar composite degradation due to wet/dry cycling.

While these results suggest that composites containing supplementary cementitious materials may exhibit improved durability to wet/dry cycling, matrix modifications in pulp fiber-cement composites have not been the subject of comprehensive evaluation to determine appropriate replacement levels for the various SCMs available for use. Also, importantly, the progressive mechanisms of composite degradation improvement have not been thoroughly examined. To date, the primary mechanism for improved composite durability has been stated as a reduction in the pore solution pH [1,5,14].

Therefore, the objectives of this research were to evaluate the performance of kraft pulp fiber-cement composites containing a variety of SCMs, at a range of dosages in binary, ternary, and quaternary blends, both prior to and after exposure to wet/dry cycling. In addition, to better understand the underlying mechanisms by which matrix modifications may affect composite durability, the microstructural and chemical changes in the composite due to supplementary cementitious material addition were examined by thermal analysis and environmental scanning electron microscopy (ESEM) with energy dispersive spectroscopy (EDS).

2. Experimental study

2.1. Materials

The 2.54 × 2.54 × 10.2 cm (1 × 1 × 4 inch) fiber-cement beams were cast with a water-to-cementitious materials ratio (w/cm) of 0.60 using commercially available ASTM Type I/II portland cement and deionized water (18.2 MΩ·m). Oxide analysis and Bogue potential composition for the cement are listed in Table 1. ADVA Flow superplasticizer, obtained from Grace Construction Products, was used at a maximum dosage rate of 6.15 mL per kilogram of cement to improve workability.

Supplementary cementitious materials (SCMs) used as a partial mass replacement for portland cement included: (1) silica fume (SF), (2) ground granulated blast furnace slag (SL), (3) Class F fly ash (FA), (4) Class C fly ash (CA), (5) metakaolin (MK), and (6) proprietary blends of raw and calcined diatomaceous earth and volcanic ash (DEVA). Force 10,000 D silica fume was obtained from Grace Construction Products. The blast furnace slag was provided by Holcim in Birmingham, AL. The two metakaolins used in this study, MK235 (Kaorock) and MK349 (Kaorock F), were provided by Thiele Kaolin Company, Sandersville, GA, and are described in detail in [15,16]. The DEVA blends were obtained from Western Pozzolan, Doyle, CA. The metakaolins and DEVA blends differ primarily in their fineness. Table 1 lists the oxide analysis of these SCMs.

Bleached, unbeaten, once-dried kraft pulp fibers were used as reinforcement at a 4% fiber volume fraction in the cement paste. The fibers were Slash Pine softwoods obtained from Buckeye Technologies in Plant City, FL. The fibers were treated

Table 1
Oxide analysis (mass percent) of ASTM Type I portland cement and supplementary cementitious materials (N/A = not available)

Oxide	Type I portland cement	Silica fume	Slag	Class F fly ash	Class C fly ash	Metakaolin (MK235)	Metakaolin (MK349)	DEVA blend (raw)	DEVA blend (calcined)
SiO_2	20.17	97.12	39.43	56.37	31.27	51.37	52.10	69.25	70.65
Al_2O_3	5.34	0.01	9.09	28.47	17.43	44.60	44.03	15.37	16.66
Fe_2O_3	3.85	0.05	0.51	6.00	6.76	0.46	0.92	5.98	5.88
CaO	63.93	0.37	35.76	1.17	28.40	0.23	0.47	1.86	1.83
MgO	0.91	0.28	12.10	1.01	5.22	0.03	0.13	0.84	0.85
Na_2O	0.05	0.04	0.16	0.24	1.62	0.39	0.02	2.01	1.87
K_2O	0.35	0.58	0.37	2.81	0.37	0.07	0.16	1.72	1.65
TiO_2	0.35	0.02	0.33	1.54	1.46	1.99	1.42	0.59	0.58
Mn_2O_3	0.08	0.04	0.56	0.04	0.08	0.01	0.01	0.07	0.06
P_2O_5	0.07	0.08	0.02	0.27	0.99	0.19	0.17	0.18	0.22
SrO	0.07	0.01	0.05	0.12	0.44	0.01	0.01	0.05	0.04
BaO	0.02	0.00	0.08	0.13	0.70	0.01	0.02	N/A	N/A
SO_3	4.00	0.04	1.55	0.05	2.81	0.16	0.00	0.31	0.10
LOI	0.80	1.36	0.01	1.79	2.45	0.51	0.56	1.65	1.59
C_3S	54.16								
C_2S	16.97								
C_3A	7.64								
C_4AF	11.70								

by a process described in [17,18] to improve their dispersion. This process involves treating the fibers with cationic starch and fly ash to improve their dispersion during mixing. The fiber volume fraction used in this research correlates to 60 g of fibers per liter of paste mix. This fiber mass does not include any fiber moisture content or starch/fly ash adsorbed to the fiber surface due to the fiber treatment.

2.2. Mechanical test methods

Paste samples were exposed to alternating wetting and drying, where a wet/dry cycle was defined as:

- 23 hours and 30 min drying in an oven at 65±5 °C and 20±5% RH;
- 30 min of air drying at 22±5 °C and 60±5% RH;
- 23 hours and 30 min soaking in water at 20±2 °C;
- 30 min of air drying at 22±5 °C and 60±5% RH; in the same manner as in [6,7].

The 2.54×2.54×10.2 cm (1×1×4 inch) samples were tested for flexural strength (first crack and peak) and post-cracking toughness according to ASTM C 348 [19] and C 293 [20]. It is important to note that all samples were tested at 78 days, regardless of the number of wet/dry cycles. All samples were cured for at least 28 days in limewater prior to cycling or mechanical testing. Thus, any variations in measured properties should be attributable to wet/dry exposure, rather than a combination of exposure and prolonged cement hydration. Similar flexure properties were seen in unexposed composites tested at 28 and 78 days.

Typical load-deflection curves for composites prior to cycling and after 25 wet/dry cycles are seen in Fig. 1. Toughness is defined here as the post-cracking toughness or the area under the load-deflection curve beyond first cracking. This definition is necessary because beams subjected to a low number of cycles exhibited load-deflection toughening after cracking, while those beams subjected to a larger number of wet/dry cycles exhibited load-deflection softening after cracking, as illustrated in [7]. In the absence of post-cracking toughening, the peak strength will be equal to the first crack strength. Peak strength values take into consideration the toughening of the composite after cracking.

2.3. Energy dispersive spectroscopy (EDS)

Microstructural observations were conducted on a FEI Quanta 200 environmental scanning electron microscope (ESEM) in a gaseous (water vapor) environment. Spectroscopy was accomplished using an EDAX SUTW detector. All EDS spectra were collected at an accelerating voltage of 10.0 kV and a water vapor pressure of 93.3 Pa (0.70 Torr). These operating conditions were chosen for the analysis of hydration products apparent on the fiber surface and within the fiber cell wall. A Monte Carlo simulation determined that this accelerating voltage (i.e., 10 kV) would produce a maximum interaction depth less than ~1.5 μm, and thereby avoid measuring any hydration products which may have formed within the fiber lumen.

EDS measurements were standardized against a blast furnace slag with a previously known chemical composition, as in [21]. The standard was compared against a synthetic ettringite sample to verify the correct quantification. Certain conditions (e.g., spot size) varied to obtain adequate ESEM images or facilitate EDS spectra collection.

Several EDS spot analyses were conducted on each observed fiber in secondary electron (SE) mode. One data point represents the average chemical composition of an observed fiber. Twenty fibers on a fracture surface of each sample type were observed.

2.4. Thermal analysis

Immediately after mechanical testing, samples were soaked in ethanol for 12 hours and oven dried at 60 °C for 24 hours. Prior to thermal analysis, samples were stored in sealed containers to minimize further cement hydration and carbonation. Samples for thermal analysis were removed from the center of the specimen fracture surfaces. Thus, any calcium carbonate found in the analysis was assumed to be indicative of carbonation after mechanical testing during sample preparation and/or subsequent storage.

Samples of approximately 30–40 mg of finely ground composite material were placed in alumina holders and maintained in a nitrogen atmosphere at a flow rate of 30 mL/min in a TA Instruments SDT 2960 DSC-TGA. Samples were heated from room temperature to approximately 1100 °C at 10 °C/min. An alumina reference holder remained empty and an oxylate "standard" was used to verify calibration.

After testing, the calcium hydroxide and calcium carbonate contents were estimated as the weight loss on the TGA curve at approximately 475 °C and 750 °C, respectively. Weight loss was determined by applying a step transition function to the leading and trailing slopes of the TGA curve about the respective weight loss temperatures (Fig. 2). All numerical calculations were conducted using TA Instruments Universal Analysis v2.5H software.

3. Mechanical test results

In this research, the effect of partial supplementary cementitious material (SCM) replacement of portland cement on the durability of kraft pulp fiber-cement composites was assessed. Results in following sections will describe the effect of SCMs on the flexural strength and toughness of the composites as a function of the number of wet/dry cycles. In this research, the maximum cement replacement for each SCM was limited only by workability. For example, silica fume replacements greater than 50% of cement could not be achieved with the maximum superplasticizer dosage rate (6.15 mL/kg) as the fresh composite mix was not flowable or cohesive. Subsequently, ternary and quaternary blends were chosen in order to optimize economical concerns, practicality, and mechanical performance. Therefore, for example, no ternary or quaternary blends were examined which contained more than 10% silica fume or metakaolin.

3.1. Silica fume (SF) replacement

Blended SF-cement composites were prepared at cement weight replacement values of 10, 30, and 50%. Prior to wet/dry cycling, first crack strengths in the SF composites (Table 2) were similar to that of the portland cement control. After the first wet/dry cycle, a decrease in first crack strength was observed for all composites. As cycling progressed, first crack strengths remained relatively unchanged for all SF composites, up to 10 cycles. Beyond 10 cycles, the 10% SF first crack strength decreased to a level comparable to the control, while the 30 and 50% SF composite first crack strengths continued to remain unchanged. After 25 cycles, the 30 and 50% SF composites exhibited 60.9% and 86.2% higher first crack strength, respectively, compared to the control.

In terms of peak strength (Table 3), degradation gradually progressed for all SF composites, up to 5 cycles. Beyond 5 cycles, the 30 and 50% SF composites exhibited no additional mechanical property losses. However, the 10% SF composite continued to show losses in peak strength. By 25 cycles, the differences between the 10% SF composite and the control were negligible. After 25 cycles, the 30 and 50% SF composite peak strength were 200.4% and 159.4% greater, respectively, than the control.

Without wet/dry exposure, post-cracking toughness values for the SF composites (Table 4), except at 50% replacement, were 35.4% and 27.4% lower for the 10 and 30% replacements than the control, respectively. The 50% replacement exhibited similar toughness as the control. After 1 wet/dry cycle, as decreases in first crack strength were seen, post-cracking toughness increased for the SF composites. After this initial increase, the rate of SF composite degradation was similar to the strength trends. That is, the 10% SF composite exhibited a gradual degradation, while the 30 and 50% SF composites did not exhibit any further observable changes. After 25 cycles, the 10% SF composite toughness was similar to that of the control. The 30% SF composite toughness was similar to that prior to cycling, while the 50% SF composite toughness showed a 34.5% increase compared to that without wet/dry exposure.

These results appear in agreement with [1,5,14]. That is, silica fume replacements of 30% or more eliminate degradation of pulp fiber-cement composites due to wet/dry cycling.

3.2. Slag (SL) replacement

SL composites were examined at 10, 30, 50, 70, and 90% replacement for portland cement by weight. Previously, slag was used at portland cement replacement values up to 70% [1,5]. Higher replacement percentages, such as 90% in this research, may improve composite durability.

Generally, as seen in Table 2, the SL composites exhibited similar first crack strength values and trends as the control both initially (i.e., at 0 cycles) and as wet/dry cycling progressed. All composites exhibited a noted decrease in first crack strength after 1 wet/dry cycle, and losses in strength continued with increasing cycles. Only the 90% SL composites did not show further first crack strength degradation following the initial decrease after 1 wet/dry cycle.

Table 3 shows that, prior to cycling, the SL composites (except for 90% SL) exhibited 23.3–37.3% lower peak strength than the control, while the 90% SL composite peak strength was comparable to the control. As cycling progressed, the peak strengths for 10–70% SL composites were generally similar to the control. Following a decrease after 1 wet/dry cycle, no further changes in the 90% SL composite peak strength were observed, and after 25 cycles, the 90% SL strength was 123.2% greater than that of the control.

As for post-cracking toughness (Table 4), the SL composites, again except for 90% SL, exhibited a slightly slower progression of degradation than the control between 1 and 5 cycles. Beyond 5 cycles, the differences between the control and the SL composites (except 90% SL) were indistinguishable. For the 90% SL composite, no observable degradation occurred over the range of wet/dry cycles. After 25 cycles, the 90% SL toughness was 8.7710 ± 3.2018 MPa mm as compared to 0.1364 ± 0.0573 MPa mm for the control.

3.3. Class F (FA) and Class C (CA) fly ash replacements

Both Class F and C fly ashes were examined at 10, 30, 50, and 70% cement replacement by weight. Both types of composites exhibited similar first crack strength results, as seen in Table 2. Prior to cycling, first crack strength decreased with increasing replacement amounts. That is, the 10% FA and CA composite first crack strengths were similar to the control, while the 70% FA and CA composite strengths were significantly less than the control even though the samples were tested at 78 days of age, suggesting the existence of an upper threshold of 10–30% for fly ash replacement for initial strength. It should be noted that the CA composite showed greater first crack strength than the FA composite, without exposure, as expected due to the latent hydraulic reactivity of Class C fly ash. By 25 cycles, both the FA and CA composites exhibited strengths similar to the control, although the rate of first crack strength degradation was slower in those composites containing fly ash.

Again, peak strength trends (Table 3) were similar to that observed with the first crack strength data. Prior to cycling, peak strength decreased with increasing replacement amounts. As with first crack strength, loss in peak strength with wet/

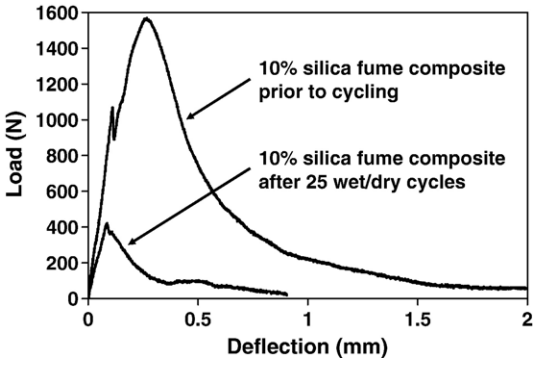

Fig. 1. Typical load-deflection curves prior to cycling and after 25 wet/dry cycles for the pulp fiber-cement composites containing SCMs.

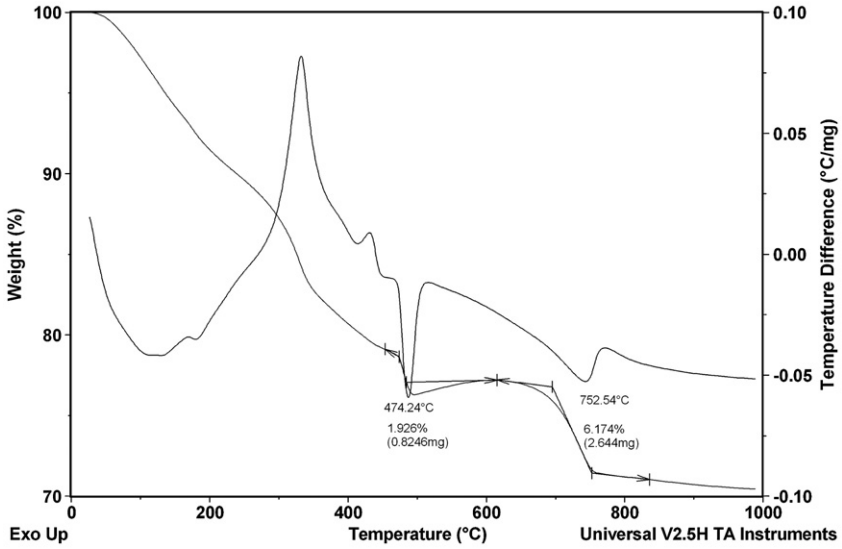

Fig. 2. Typical TGA-DTA curve for pulp fiber-cement composite with example calculation of calcium hydroxide (~475 °C) and calcium carbonate (~750 °C) mass loss percentages.

dry cycling was slower in the FA and CA composites than the control. However, by 25 wet/dry cycles, peak strength differences between the fly ash and the control composites were negligible.

In terms of post-cracking toughness (Table 4), all fly ash composites prior to cycling, except for the 10 and 30% CA composites, showed lower toughness that the control. With wetting and drying, all FA/CA composites exhibited a slower rate of degradation than the control. Contrary to the strength trends, increasing replacement amounts led to improvements in toughness with wet/dry cycling. However, after 25 cycles, only the 70% FA/CA composite toughness was greater than the

Table 2
First crack strength (MPa) of binary SCM kraft pulp fiber-cement composites as a function of the number of wet/dry cycles

	Number of wet/dry cycles													
Sample characteristics	0		1		2		5		10		15		25	
Control	5.95	(0.32)	3.51	(0.47)	3.39	(0.52)	2.25	(0.72)	2.63	(0.26)	2.83	(0.33)	2.85	(0.59)
10% SF	6.90	(0.72)	5.61	(0.51)	5.55	(0.93)	4.46	(0.60)	4.42	(0.10)	3.36	(0.02)	3.12	(0.21)
30% SF	6.39	(0.34)	5.05	(0.54)	5.82	(0.63)	5.39	(0.89)	5.13	(0.65)	5.12	(0.92)	4.59	(0.52)
50% SF	6.03	(0.34)	4.65	(0.39)	4.78	(0.54)	5.01	(0.99)	5.34	(1.45)	4.78	(0.75)	5.32	(0.92)
10% SL	5.80	(0.32)	5.00	(0.31)	4.90	(0.11)	3.90	(0.33)	4.26	(0.43)	3.47	(0.35)	1.69	(0.07)
30% SL	5.41	(0.45)	3.85	(0.70)	3.46	(0.16)	3.95	(0.42)	2.71	(0.18)	2.44	(0.24)	1.92	(0.56)
50% SL	5.58	(0.53)	3.36	(0.09)	3.20	(0.42)	2.40	(0.49)	2.26	(0.17)	2.14	(0.16)	1.91	(0.10)
70% SL	5.21	(0.23)	3.36	(0.33)	3.25	(0.12)	2.64	(0.62)	2.10	(0.30)	2.16	(0.31)	1.65	(0.06)
90% SL	6.14	(0.33)	3.34	(0.50)	3.13	(0.40)	3.09	(0.39)	3.29	(0.33)	3.18	(0.25)	3.32	(0.89)
10% CA	5.77	(0.35)	5.79	(0.44)	5.31	(0.20)	4.95	(0.93)	3.93	(0.39)	3.47	(0.06)	3.81	(0.66)
30% CA	5.18	(0.40)	6.22	(1.59)	6.54	(1.09)	6.80	(0.90)	5.67	(0.66)	6.45	(0.59)	3.94	(0.93)
50% CA	3.95	(0.13)	3.13	(0.42)	2.94	(0.41)	3.65	(0.57)	3.63	(0.41)	3.60	(0.36)	2.39	(0.35)
70% CA	3.78	(0.61)	2.59	(0.27)	2.75	(0.10)	2.78	(0.67)	2.86	(0.54)	2.51	(0.41)	2.45	(0.16)
10% FA	5.76	(0.45)	5.44	(0.14)	5.43	(0.46)	4.79	(0.44)	4.24	(0.20)	4.29	(0.67)	3.53	(0.41)
30% FA	4.75	(0.44)	4.54	(0.50)	4.62	(0.40)	4.50	(0.09)	4.37	(0.12)	3.61	(0.21)	3.43	(0.68)
50% FA	3.76	(0.21)	2.85	(0.12)	3.13	(0.33)	3.37	(0.13)	2.59	(0.35)	2.46	(0.32)	2.59	(0.21)
70% FA	2.15	(0.39)	2.04	(0.21)	1.75	(0.15)	1.59	(0.10)	1.98	(0.47)	1.70	(0.08)	1.62	(0.37)
10% MK235	5.05	(0.24)	4.96	(0.95)	3.58	(0.75)	3.05	(0.55)	2.90	(0.57)	2.42	(0.95)	2.69	(0.42)
30% MK235	4.51	(0.21)	7.04	(2.22)	6.75	(0.62)	5.66	(1.07)	6.14	(0.38)	5.55	(0.68)	5.24	(0.19)
10% MK349	5.55	(0.35)	3.98	(0.68)	2.91	(0.44)	2.28	(0.49)	1.91	(0.09)	2.09	(0.31)	1.83	(0.33)
30% MK349	4.50	(0.82)	3.69	(0.49)	2.83	(0.12)	4.60	(0.76)	4.10	(0.78)	3.63	(0.57)	2.54	(0.22)
10% DEVA calcined	5.88	(0.46)	5.45	(0.63)	4.52	(0.38)	4.78	(0.70)	4.54	(0.42)	4.88	(0.05)	4.00	(0.14)
30% DEVA calcined	5.96	(0.15)	4.69	(0.42)	5.21	(0.41)	4.95	(0.51)	4.46	(0.72)	3.49	(0.04)	3.46	(0.29)
50% DEVA calcined	5.11	(0.48)	4.24	(0.65)	4.87	(0.82)	5.10	(0.50)	4.49	(0.53)	4.75	(0.93)	3.94	(0.92)
10% DEVA raw	5.99	(0.77)	6.30	(0.33)	6.23	(0.28)	5.69	(0.16)	4.89	(0.59)	4.83	(0.24)	3.98	(0.59)
30% DEVA raw	5.70	(0.40)	6.03	(1.10)	5.13	(0.61)	4.52	(0.34)	3.60	(0.35)	3.16	(0.57)	2.39	(0.54)
50% DEVA raw	4.33	(0.58)	2.80	(0.46)	5.31	(0.36)	4.21	(0.63)	4.36	(0.86)	4.66	(0.92)	4.55	(1.43)

Note: the number in parentheses indicates one standard deviation for each average.

Table 3
Peak strength (MPa) of binary SCM kraft pulp fiber-cement composites as a function of the number of wet/dry cycles

	Number of wet/dry cycles													
Sample characteristics	0		1		2		5		10		15		25	
Control	10.34	(0.36)	5.80	(1.03)	3.83	(0.13)	2.25	(0.72)	2.63	(0.26)	2.83	(0.33)	2.85	(0.59)
10% SF	10.48	(1.25)	10.07	(0.09)	8.53	(0.84)	7.37	(1.27)	4.82	(0.10)	3.36	(0.02)	3.12	(0.21)
30% SF	11.62	(1.21)	10.58	(2.55)	9.26	(1.23)	8.58	(0.13)	8.63	(0.55)	7.78	(0.68)	8.57	(1.00)
50% SF	9.84	(0.53)	8.95	(1.26)	8.70	(1.12)	7.29	(0.86)	8.49	(0.89)	7.00	(0.11)	7.40	(0.39)
10% SL	7.72	(0.87)	5.87	(0.96)	5.95	(0.77)	3.91	(0.35)	4.26	(0.43)	3.47	(0.35)	1.69	(0.07)
30% SL	7.63	(1.04)	4.76	(1.01)	4.85	(0.25)	3.95	(0.42)	2.71	(0.18)	2.44	(0.24)	1.92	(0.56)
50% SL	6.48	(1.36)	4.84	(0.66)	3.75	(0.47)	2.84	(0.27)	2.70	(0.31)	2.14	(0.16)	1.91	(0.10)
70% SL	7.94	(0.83)	5.54	(0.49)	4.68	(0.43)	3.53	(0.63)	2.60	(0.40)	2.76	(0.32)	1.98	(0.12)
90% SL	9.84	(1.41)	5.75	(1.06)	5.46	(0.75)	5.50	(1.20)	5.45	(0.87)	6.06	(0.79)	6.37	(1.77)
10% CA	9.77	(0.61)	7.97	(1.10)	7.42	(1.14)	4.96	(0.92)	3.93	(0.39)	3.47	(0.06)	3.81	(0.66)
30% CA	10.52	(1.27)	9.11	(1.51)	9.00	(1.72)	7.63	(1.01)	5.91	(0.63)	6.45	(0.59)	3.94	(0.93)
50% CA	6.33	(0.71)	5.00	(0.41)	5.22	(0.96)	5.10	(0.98)	3.79	(0.28)	3.60	(0.36)	2.39	(0.35)
70% CA	6.10	(0.99)	4.27	(0.58)	4.74	(0.38)	4.91	(1.13)	3.95	(0.33)	3.65	(0.28)	3.21	(0.39)
10% FA	8.73	(0.83)	8.16	(1.22)	8.16	(0.32)	5.06	(0.38)	4.24	(0.20)	4.29	(0.67)	3.53	(0.41)
30% FA	8.39	(0.76)	7.56	(1.37)	7.83	(1.27)	6.92	(0.22)	4.75	(0.33)	3.61	(0.21)	3.43	(0.68)
50% FA	6.08	(0.78)	4.86	(0.57)	5.27	(0.78)	5.22	(0.21)	3.72	(0.32)	2.82	(0.52)	2.59	(0.21)
70% FA	3.82	(0.30)	3.36	(0.02)	3.47	(0.17)	3.15	(0.23)	3.29	(0.33)	2.68	(0.28)	2.67	(0.72)
10% MK235	9.72	(0.85)	9.59	(0.62)	8.04	(1.73)	5.30	(0.74)	3.53	(0.13)	2.42	(0.95)	2.69	(0.42)
30% MK235	9.92	(1.14)	9.96	(2.19)	9.38	(2.10)	9.29	(1.09)	10.48	(0.46)	9.65	(1.60)	9.05	(0.43)
10% MK349	9.98	(0.90)	8.42	(0.86)	6.10	(0.45)	3.79	(1.43)	2.19	(0.08)	2.09	(0.31)	1.83	(0.33)
30% MK349	9.35	(1.71)	9.11	(1.12)	9.13	(1.72)	11.02	(1.47)	9.20	(0.47)	9.08	(1.04)	4.71	(0.69)
10% DEVA calcined	9.94	(0.90)	8.94	(0.19)	7.74	(1.45)	5.71	(0.63)	4.54	(0.42)	4.88	(0.05)	4.00	(0.14)
30% DEVA calcined	8.28	(0.64)	7.24	(1.17)	7.91	(0.41)	6.43	(0.84)	5.46	(0.48)	3.64	(0.14)	3.46	(0.29)
50% DEVA calcined	7.69	(0.86)	6.86	(1.21)	7.82	(0.82)	9.38	(1.30)	7.53	(1.55)	6.61	(0.50)	5.79	(0.49)
10% DEVA raw	9.88	(1.24)	9.53	(0.85)	9.12	(2.17)	6.12	(0.32)	4.89	(0.59)	4.83	(0.24)	3.98	(0.59)
30% DEVA raw	8.92	(1.18)	9.19	(1.41)	9.09	(1.07)	7.55	(0.49)	3.72	(0.46)	3.16	(0.57)	2.39	(0.54)
50% DEVA raw	7.44	(0.84)	6.41	(0.65)	8.33	(0.74)	6.86	(0.99)	7.32	(1.59)	6.18	(1.42)	6.33	(1.40)

Note: the number in parentheses indicates one standard deviation for each average.

control. In addition, the 70% FA composite toughness was greater than that of the 70% CA composite. However, the toughness of both 70% fly ash composites was significantly less than that of the control prior to cycling.

3.4. Metakaolin (MK235 and MK349) replacement

Two metakaolins were evaluated at cement replacement values of 10 and 30%. These samples, denoted MK235 and MK349, differ primarily in their surface area. MK235 has a surface area of 11.1 m^2/g, while MK349 has a surface area of 25.4 m^2/g. MK349 has been shown [16] to generally be more reactive, producing higher flexural and compressive strength and at earlier ages than the MK235.

Prior to cycling (Table 2), it was observed that the MK composites exhibited 6.7–24.3% lower first crack strength than the control. In addition, for both types of MK, the 30% composite first crack strength was lower than the 10% composite. Over the range of wet/dry cycles investigated here, the 10% MK235 and both MK349 first crack strengths were similar to the control. However, the 30% MK349 exhibited a noticeable increase in strength between 2 and 5 cycles, although strength decreased with additional cycling. After 1 wet/dry cycle, the 30% MK235 composite exhibited a 56.3% increase in first crack strength. By 25 cycles, the 30% MK235 composite first crack strength was comparable to the control prior to cycling. However, all other metakaolin composites exhibited similar strengths as the control.

Table 3 illustrates the MK peak strength results. Without wet/dry exposure, all MK composites showed similar peak strength values as the control. No changes in strength were observed after 1 wet/dry cycle, but additional cycling led to decreases in peak strength for both 10% MK composites. By 10 cycles, the 10% MK composite peak strength were comparable to that of the control. The 30% MK composites exhibited negligible changes, up to 15 cycles. After 25 cycles, the 30% MK349 composite exhibited a 43.5% decrease in peak strength. However, the 30% MK235 composite, over the range of wet/dry cycles investigated here, did not exhibit any composite peak strength degradation.

Post-cracking toughness results (Table 4) show that, prior to cycling, the MK235 composites exhibited lower toughness than the control, while the MK349 composite toughness was similar to the control. With progressive cycling, the 10% MK toughness values decreased significantly following a slight increase after 1 wet/dry cycle. Up to 5 cycles, the 30% MK composites did not exhibit any degradation. However, beyond 5 cycles, the 30% MK349 toughness decreased, while the 30% MK235 toughness remained unchanged. After 25 cycles, the 30% MK235 composite toughness was comparable to the control prior to cycling.

3.5. DEVA blend (raw and calcined) replacement

Commercially available, proprietary blends of diatomaceous earth and volcanic ash were examined at 10, 30, and 50% replacements by weight of cement and differed primarily in

Table 4
Post-cracking toughness (MPa mm) of binary SCM kraft pulp fiber-cement composites as a function of the number of wet/dry cycles

Sample characteristics	Number of wet/dry cycles													
	0		1		2		5		10		15		25	
Control	8.57	(2.15)	3.29	(0.24)	0.69	(0.16)	0.17	(0.09)	0.10	(0.04)	0.11	(0.05)	0.11	(0.06)
10% SF	5.54	(0.95)	7.86	(1.28)	4.74	(1.62)	2.48	(0.73)	0.77	(0.11)	0.41	(0.10)	0.39	(0.22)
30% SF	6.22	(1.41)	7.47	(1.72)	6.37	(1.73)	5.93	(0.51)	7.83	(0.70)	6.77	(0.77)	5.99	(0.28)
50% SF	7.93	(1.21)	11.33	(3.86)	9.47	(2.13)	9.64	(3.95)	7.90	(0.09)	8.76	(0.32)	10.67	(2.99)
10% SL	5.48	(0.54)	3.95	(0.74)	2.59	(0.29)	0.69	(0.09)	0.27	(0.03)	0.16	(0.08)	0.08	(0.03)
30% SL	5.43	(1.12)	3.04	(0.82)	2.20	(0.29)	0.82	(0.06)	0.23	(0.05)	0.19	(0.03)	0.12	(0.03)
50% SL	4.55	(1.14)	3.56	(0.92)	2.08	(0.17)	0.65	(0.06)	0.62	(0.05)	0.32	(0.03)	0.40	(0.11)
70% SL	5.99	(1.27)	4.79	(1.11)	3.61	(0.55)	1.30	(0.34)	0.69	(0.08)	0.69	(0.07)	0.69	(0.18)
90% SL	8.97	(1.83)	7.95	(2.44)	7.00	(1.30)	6.61	(2.10)	7.07	(1.38)	7.02	(0.97)	8.77	(3.20)
10% CA	10.10	(0.89)	6.19	(0.12)	4.93	(1.35)	1.30	(0.17)	0.45	(0.17)	0.29	(0.05)	0.21	(0.04)
30% CA	12.42	(0.89)	7.86	(1.47)	5.95	(1.70)	1.97	(0.30)	0.97	(0.19)	0.42	(0.05)	0.21	(0.02)
50% CA	3.94	(0.58)	3.81	(0.58)	3.33	(0.51)	2.00	(0.76)	0.58	(0.17)	0.44	(0.14)	0.18	(0.07)
70% CA	4.31	(1.14)	2.92	(0.28)	3.52	(0.77)	3.57	(1.00)	2.20	(0.72)	1.95	(0.17)	1.37	(0.34)
10% FA	5.34	(0.47)	4.77	(0.40)	3.29	(0.80)	1.12	(0.08)	0.31	(0.07)	0.22	(0.03)	0.16	(0.05)
30% FA	5.74	(0.79)	5.28	(1.21)	5.03	(1.74)	2.94	(0.40)	0.56	(0.08)	0.33	(0.06)	0.30	(0.13)
50% FA	4.42	(1.04)	3.58	(0.62)	4.11	(0.80)	2.97	(0.57)	0.94	(0.14)	0.78	(0.04)	0.44	(0.11)
70% FA	5.42	(0.99)	5.20	(0.78)	5.63	(0.86)	5.07	(1.19)	4.16	(0.62)	3.41	(0.25)	3.39	(1.64)
10% MK235	5.80	(1.12)	7.60	(0.93)	5.24	(1.61)	1.45	(0.62)	0.56	(0.25)	0.17	(0.04)	0.20	(0.05)
30% MK235	6.04	(0.84)	7.88	(1.77)	7.25	(1.83)	8.37	(2.02)	7.12	(1.39)	6.52	(0.41)	7.32	(1.11)
10% MK349	9.48	(1.37)	10.84	(2.21)	5.61	(1.94)	1.53	(0.61)	0.45	(0.08)	0.25	(0.05)	0.21	(0.06)
30% MK349	7.30	(2.74)	8.05	(1.67)	7.71	(1.32)	10.33	(1.59)	5.24	(0.62)	4.60	(1.25)	1.57	(0.22)
10% DEVA calcined	8.69	(2.35)	6.81	(0.97)	7.24	(1.97)	2.93	(0.97)	0.69	(0.30)	0.26	(0.04)	0.18	(0.02)
30% DEVA calcined	6.50	(0.62)	7.82	(2.15)	7.63	(1.22)	5.05	(0.78)	2.04	(0.33)	1.03	(0.08)	0.65	(0.18)
50% DEVA calcined	6.08	(0.78)	8.44	(1.82)	8.14	(0.76)	9.92	(1.47)	8.10	(2.13)	5.22	(0.79)	4.65	(0.35)
10% DEVA raw	5.43	(0.56)	5.61	(0.81)	4.87	(0.71)	1.30	(0.08)	0.43	(0.17)	0.23	(0.11)	0.17	(0.05)
30% DEVA raw	6.01	(0.67)	6.99	(0.98)	7.46	(0.63)	3.40	(0.99)	0.69	(0.07)	0.49	(0.10)	0.74	(0.16)
50% DEVA raw	7.50	(0.82)	10.00	(0.71)	8.65	(2.13)	5.87	(1.72)	5.36	(1.68)	3.31	(1.05)	3.78	(1.02)

Note: the number in parentheses indicates one standard deviation for each average.

their surface area. The raw blend had a larger surface area (2.654 m^2/g) than the calcined blend (0.999 m^2/g).

As with the fly ash samples, the different DEVA blends exhibited similar results. For both first crack strength (Table 2) and peak strength (Table 3), increasing replacement amounts led to lower strengths. While all DEVA replacements did slow the progression of strength degradation as compared to the control, by 25 cycles DEVA strengths were similar to the control. Only the 50% DEVA composites exhibited significantly greater (102.9–121.7%) peak strength than the control.

Table 5
First crack strength (MPa) of ternary and quaternary SCM kraft pulp fiber-cement composites as a function of the number of wet/dry cycles

Sample characteristics	Number of wet/dry cycles													
	0		1		2		5		10		15		25	
Control	5.95	(0.32)	3.51	(0.47)	3.39	(0.52)	2.25	(0.72)	2.63	(0.26)	2.83	(0.33)	2.85	(0.59)
10% SF/30% CA	4.13	(0.14)	3.16	(0.19)	2.73	(0.46)	2.40	(0.35)	2.36	(0.20)	2.58	(0.27)	2.33	(0.46)
10% SF/30% FA	4.19	(0.54)	3.66	(0.47)	3.65	(0.06)	3.15	(0.40)	3.03	(0.31)	2.49	(0.14)	2.33	(0.39)
10% SF/30% SL	4.70	(0.39)	5.34	(0.43)	4.89	(1.63)	3.49	(0.85)	2.88	(0.17)	2.02	(0.23)	2.14	(0.67)
10% SF/50% SL	5.92	(0.51)	4.68	(0.13)	4.13	(0.35)	3.56	(0.10)	3.07	(0.46)	2.99	(0.05)	3.16	(0.52)
10% SF/70% SL	7.04	(0.36)	4.82	(0.33)	4.82	(0.33)	5.20	(0.36)	3.40	(0.11)	3.38	(0.40)	3.42	(0.33)
10% SF/10% MK235	5.26	(0.29)	5.00	(0.66)	4.86	(0.50)	3.77	(0.47)	2.56	(0.45)	2.69	(0.06)	2.25	(0.42)
10% SF/10% MK349	4.49	(0.20)	3.56	(0.32)	3.36	(0.18)	2.69	(0.46)	2.85	(0.17)	2.17	(0.38)	2.67	(0.43)
10% MK235/30% SL	4.91	(0.35)	4.05	(0.30)	4.01	(0.47)	2.80	(0.06)	1.75	(0.15)	1.54	(0.05)	1.27	(0.33)
10% MK235/70% SL	5.10	(0.48)	4.06	(0.21)	3.56	(0.15)	4.25	(0.16)	4.31	(0.37)	3.76	(0.26)	3.28	(0.15)
10% CA/30% SL	5.14	(0.68)	3.47	(0.13)	3.48	(0.15)	2.86	(0.45)	2.49	(0.38)	1.68	(0.39)	1.74	(0.22)
10% CA/50% SL	5.16	(0.28)	3.84	(0.28)	3.20	(0.38)	2.90	(0.16)	2.44	(0.53)	1.94	(0.72)	2.48	(0.13)
30% CA/30% SL	3.37	(0.04)	2.85	(0.16)	2.72	(0.56)	2.43	(0.09)	2.44	(0.35)	2.19	(0.23)	2.07	(0.47)
10% FA/30% SL	5.07	(0.36)	3.06	(0.25)	2.93	(0.28)	2.79	(0.42)	2.22	(0.58)	1.95	(0.19)	1.41	(0.21)
10% FA/50% SL	5.20	(0.68)	3.54	(0.40)	2.92	(0.09)	1.70	(0.32)	1.98	(0.16)	2.31	(0.30)	1.92	(0.26)
30% FA/30% SL	3.61	(0.15)	3.37	(0.13)	3.20	(0.03)	2.69	(0.47)	1.63	(0.27)	2.01	(0.13)	1.54	(0.02)
10% MK235/10% SF/30% SL	4.81	(0.38)	4.13	(0.39)	3.88	(0.44)	4.18	(0.40)	2.71	(0.06)	2.43	(0.13)	2.13	(0.16)
10% MK235/10% SF/50% SL	4.51	(0.46)	4.40	(0.18)	4.60	(0.54)	4.64	(0.35)	4.05	(0.22)	3.62	(0.20)	3.90	(0.31)
10% MK235/10% SF/70% SL	5.01	(0.24)	4.54	(0.20)	4.34	(0.49)	4.35	(0.47)	5.11	(0.17)	4.75	(0.46)	4.80	(0.28)

Note: the number in parentheses indicates one standard deviation for each average.

Table 6
Peak strength (MPa) of ternary and quaternary SCM kraft pulp fiber-cement composites as a function of the number of wet/dry cycles

Sample characteristics	Number of wet/dry cycles													
	0		1		2		5		10		15		25	
Control	10.34	(0.36)	5.80	(1.03)	3.83	(0.13)	2.25	(0.72)	2.63	(0.26)	2.83	(0.33)	2.85	(0.59)
10% SF/30% CA	8.04	(0.65)	7.96	(1.08)	6.66	(0.90)	5.65	(0.70)	3.10	(0.32)	2.62	(0.27)	2.50	(0.64)
10% SF/30% FA	7.22	(1.17)	7.26	(0.70)	7.24	(0.80)	5.01	(0.71)	3.10	(0.28)	2.49	(0.14)	2.33	(0.39)
10% SF/30% SL	9.82	(0.84)	7.45	(0.84)	6.92	(1.55)	4.42	(0.36)	2.88	(0.17)	2.02	(0.23)	2.14	(0.67)
10% SF/50% SL	11.74	(0.66)	9.44	(0.70)	8.41	(1.04)	8.19	(1.33)	6.06	(0.59)	4.68	(0.86)	3.95	(0.50)
10% SF/70% SL	11.91	(0.95)	9.29	(0.47)	8.39	(1.14)	8.60	(0.61)	7.72	(0.80)	7.67	(0.78)	6.47	(0.33)
10% SF/10% MK235	9.46	(0.89)	9.46	(2.20)	9.40	(1.25)	5.79	(1.17)	2.98	(0.41)	2.69	(0.06)	2.25	(0.42)
10% SF/10% MK349	9.38	(1.32)	7.80	(0.49)	7.49	(0.37)	4.36	(0.25)	3.41	(0.38)	2.22	(0.43)	2.67	(0.43)
10% MK235/30% SL	8.84	(1.75)	7.94	(0.56)	7.74	(0.82)	3.44	(0.27)	2.01	(0.40)	1.54	(0.05)	1.27	(0.33)
10% MK235/70% SL	8.12	(0.74)	7.67	(0.36)	7.44	(0.32)	8.26	(0.02)	9.01	(0.84)	6.78	(0.72)	6.01	(0.72)
10% CA/30% SL	9.68	(1.24)	6.65	(0.43)	5.86	(0.61)	3.46	(0.35)	2.52	(0.35)	1.68	(0.39)	1.74	(0.22)
10% CA/50% SL	9.58	(0.53)	8.00	(0.72)	6.48	(0.83)	3.66	(0.19)	2.51	(0.47)	1.94	(0.72)	2.48	(0.13)
30% CA/30% SL	5.89	(0.82)	5.55	(0.83)	4.90	(0.84)	2.49	(0.16)	2.44	(0.35)	2.19	(0.23)	2.07	(0.47)
10% FA/30% SL	9.52	(1.16)	6.20	(0.49)	5.60	(0.54)	2.99	(0.21)	2.22	(0.58)	1.95	(0.19)	1.41	(0.21)
10% FA/50% SL	9.53	(1.95)	7.40	(0.90)	6.02	(1.40)	3.04	(0.54)	1.98	(0.16)	2.31	(0.30)	1.92	(0.26)
30% FA/30% SL	6.88	(0.87)	6.34	(0.42)	6.03	(0.59)	3.22	(0.66)	1.70	(0.27)	2.06	(0.04)	1.54	(0.02)
10% MK235/10% SF/30% SL	10.54	(0.94)	8.26	(1.31)	7.99	(0.95)	6.44	(1.12)	3.70	(0.26)	3.00	(0.36)	3.07	(0.22)
10% MK235/10% SF/50% SL	9.49	(0.59)	8.75	(0.40)	11.51	(2.05)	10.48	(0.47)	9.21	(1.86)	7.94	(0.89)	5.72	(0.20)
10% MK235/10% SF/70% SL	8.16	(0.42)	7.31	(0.45)	7.09	(0.49)	8.12	(0.84)	7.97	(1.32)	7.87	(0.50)	7.99	(0.86)

Note: the number in parentheses indicates one standard deviation for each average.

Up to 2 wet/dry cycles, the DEVA composites did not exhibit considerable changes in post-cracking toughness as seen in Table 4. Beyond this point, all DEVA composites showed decreases in toughness. After 25 cycles, only the 50% DEVA composites showed improved toughness as compared to the control. However, these toughness values were 45.8–55.9% lower than that of the control prior to cycling.

3.6. Ternary and quaternary blend replacements

Ternary and quaternary SCM blends were also investigated in order to consider economy as well as performance. For example, though the 30 and 50% SF composites showed no signs of degradation, these replacement values are not commercially practical due to poor workability and finishability and will have a significantly increased cost. Thus, blends of fly ash/slag, silica fume/slag, silica fume/fly ash, metakaolin/slag, metakaolin/silica fume, and metakaolin/silica fume/slag were investigated.

Results for these SCM blended kraft pulp fiber-cement composites are shown in Tables 5–7. It can be seen that the fly ash/slag, silica fume/fly ash, and metakaolin/silica fume blends did not produce results that would indicate these ternary blends were effective in mitigating damage due to wet/dry cycling.

Table 7
Post-cracking toughness (MPa mm) of ternary and quaternary SCM kraft pulp fiber-cement composites as a function of the number of wet/dry cycles

Sample characteristics	Number of wet/dry cycles													
	0		1		2		5		10		15		25	
Control	8.57	(2.15)	3.29	(0.24)	0.69	(0.16)	0.17	(0.09)	0.10	(0.04)	0.11	(0.05)	0.11	(0.06)
10% SF/30% CA	4.58	(0.22)	6.11	(2.04)	4.02	(1.48)	2.39	(0.57)	0.70	(0.10)	2.76	(0.16)	0.36	(0.22)
10% SF/30% FA	3.93	(0.69)	5.03	(1.10)	4.78	(1.11)	1.95	(0.39)	0.33	(0.07)	0.20	(0.06)	0.21	(0.05)
10% SF/30% SL	8.22	(0.42)	8.13	(0.64)	5.91	(1.44)	2.10	(0.93)	0.74	(0.26)	0.38	(0.06)	0.47	(0.15)
10% SF/50% SL	5.58	(0.76)	6.67	(1.75)	5.71	(0.93)	5.30	(1.96)	2.42	(0.51)	1.52	(0.26)	1.11	(0.20)
10% SF/70% SL	6.54	(0.39)	7.38	(0.86)	6.84	(2.36)	6.34	(0.95)	6.26	(0.92)	6.12	(1.23)	5.62	(0.50)
10% SF/10% MK235	5.19	(0.86)	6.28	(1.49)	6.69	(0.76)	1.61	(0.57)	0.41	(0.04)	0.26	(0.08)	0.17	(0.01)
10% SF/10% MK349	5.65	(1.62)	5.31	(1.15)	4.30	(0.40)	1.45	(0.12)	0.61	(0.10)	0.21	(0.08)	0.15	(0.01)
10% MK235/30% SL	6.00	(1.71)	5.62	(0.78)	4.81	(0.65)	0.82	(0.15)	0.42	(0.16)	0.25	(0.06)	0.26	(0.01)
10% MK235/70% SL	5.35	(1.03)	7.99	(2.19)	6.95	(1.86)	6.99	(0.79)	5.84	(1.44)	3.28	(0.59)	2.58	(0.59)
10% CA/30% SL	9.16	(1.42)	5.34	(0.65)	3.02	(0.60)	1.09	(0.38)	0.24	(0.04)	0.13	(0.07)	0.27	(0.20)
10% CA/50% SL	6.65	(1.01)	5.10	(1.11)	3.25	(0.66)	0.73	(0.12)	0.32	(0.07)	0.32	(0.12)	0.29	(0.06)
30% CA/30% SL	7.29	(1.45)	6.81	(1.74)	3.47	(0.83)	0.54	(0.16)	0.59	(0.23)	0.36	(0.17)	0.46	(0.06)
10% FA/30% SL	8.42	(1.64)	5.68	(0.80)	2.90	(0.66)	0.66	(0.15)	0.17	(0.02)	0.21	(0.04)	0.15	(0.04)
10% FA/50% SL	5.09	(1.96)	6.93	(1.58)	2.20	(1.18)	0.87	(0.20)	2.57	(0.13)	0.34	(0.05)	0.37	(0.18)
30% FA/30% SL	5.27	(1.06)	4.71	(0.60)	2.61	(0.22)	0.47	(0.10)	0.40	(0.22)	0.42	(0.02)	0.17	(0.06)
10% MK235/10% SF/30% SL	7.32	(1.76)	7.02	(2.16)	6.18	(1.26)	3.29	(0.26)	1.30	(0.30)	1.01	(0.34)	1.10	(0.23)
10% MK235/10% SF/50% SL	6.32	(1.81)	7.60	(1.35)	10.68	(2.51)	8.87	(0.74)	5.48	(1.14)	4.28	(0.64)	2.67	(0.50)
10% MK235/10% SF/70% SL	7.10	(0.33)	8.42	(2.50)	8.27	(1.70)	7.97	(1.49)	8.48	(1.12)	7.61	(1.55)	8.28	(2.57)

Note: the number in parentheses indicates one standard deviation for each average.

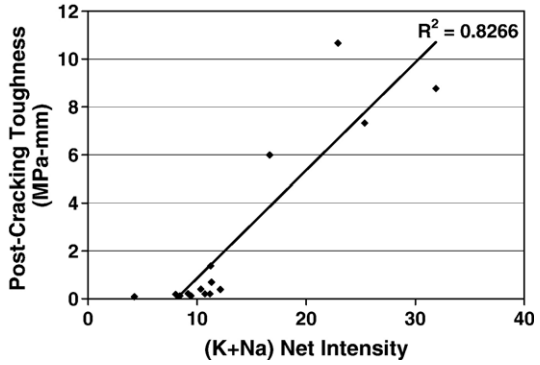

Fig. 3. Effect of alkali content ([K+Na] net intensity) on composite post-cracking toughness after 25 wet/dry cycles (MPa mm).

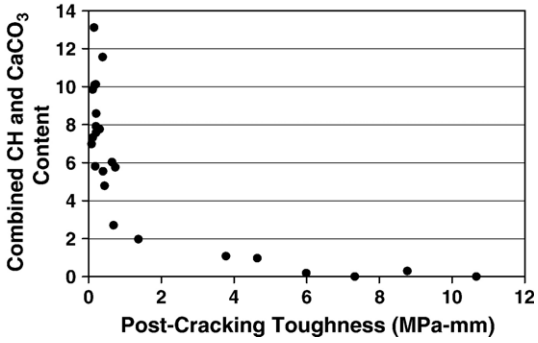

Fig. 5. Effect of combined calcium hydroxide and calcium carbonate content, measured prior to cycling, on composite post-cracking toughness, measured after 25 wet/dry cycles (MPa mm).

However, results show that the 10% SF/70% SL and 10% MK235/70% SL composites minimized the progression of composite degradation during wet/dry cycling. The 10% MK235/10% SF/70% SL quaternary blend composite did not exhibit any signs of composite degradation over the range of wet/dry cycles investigated in this study. After 25 cycles, first crack and peak strengths for the blended composite were 19.3% and 22.7% lower, respectively, than the control without exposure. Toughness, after 25 cycles, for the quaternary blend composite was similar to the unexposed control.

4. Microstructural characterization and chemical analysis

To better understand the underlying mechanisms of damage and the influence of the SCMs on the structure and performance of the composites, ESEM with EDS and thermogravimetric analysis (TGA) were performed on fractured surfaces and ground samples, respectively. Samples were selected to provide a representation of those unaffected by SCM replacement as well as those which showed improvements in composite durability.

4.1. Alkali content

ESEM EDS analysis performed on the kraft pulp fiber surfaces revealed that the replacement of portland cement with SCMs maintained and/or increased the apparent alkali content on the fiber surfaces. That is, after 25 wet/dry cycles, the alkali contents (as measured by EDS net intensity) on the fiber surfaces and/or within the fiber cell walls of the SCM-containing composites were similar to or greater than the control (without SCMs) prior to cycling. In addition, the alkali content and composite flexural toughness after 25 cycles appear to be directly related, as seen in Fig. 3. Thus, the increased stability of alkalis (i.e., decreased leaching) during wet/dry

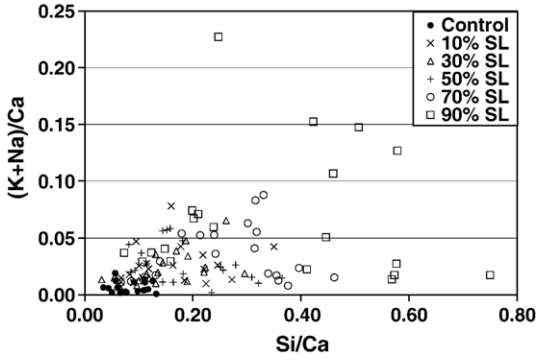

Fig. 4. Average alkali content ([K+Na]/Ca) versus average Si/Ca molar ratio for kraft pulp fiber-cement composites containing slag after 25 wet/dry cycles.

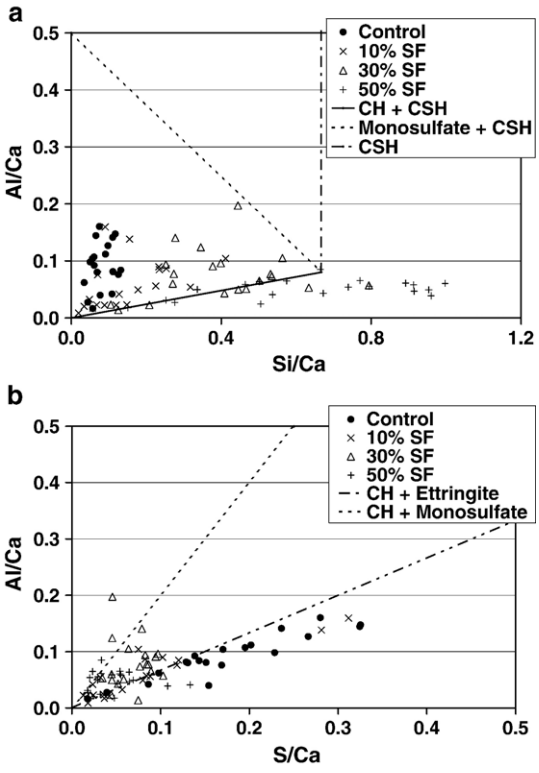

Fig. 6. Effect of silica fume on kraft fiber surface and cell wall chemical composition after 25 wet/dry cycles. (a) Average Al/Ca versus Si/Ca molar ratios. Note: the solid, short dashed, and long dashed lines represent the theoretical compositions of CH intermixed with C–S–H, monosulfate intermixed with C–S–H, and C–S–H, respectively. (b) Average Al/Ca versus S/Ca molar ratios. Note: the short dashed and long dashed lines represent the theoretical compositions of CH intermixed with monosulfate and CH intermixed with ettringite, respectively.

cycling seems to improve resistance to degradation, possibly by buffering the pore solution.

Wet/dry cycling has been shown to result in alkali leaching from pure portland cement pulp fiber-cement composites [10]. Monosulfate aluminate hydrate is believed to be destabilized during alkali leaching, leading to the formation of ettringite (i.e., delayed/secondary ettringite formation) [22,23]. Secondary ettringite formation has been previously suggested as one of the mechanisms of pulp fiber-cement degradation [7,10]. Thus, it is suggested that the incorporation of SCMs contributes to improved composite durability by reducing alkali leaching (i.e., favoring monosulfate stabilization). It is believed that the formation of supplementary C–S–H leads to increased adsorption of alkalis. Fig. 4 illustrates an example of increased alkali content with increased Si/Ca ratios (i.e., increased formation and abundance of supplementary C–S–H) using slag as a SCM. This theory is similar to the mechanisms of alkali–silica reaction (ASR) control by the use of SCMs. For ASR, supplementary C–S–H binds alkalis through the formation of non-expansive C–N(K)–S–H [24].

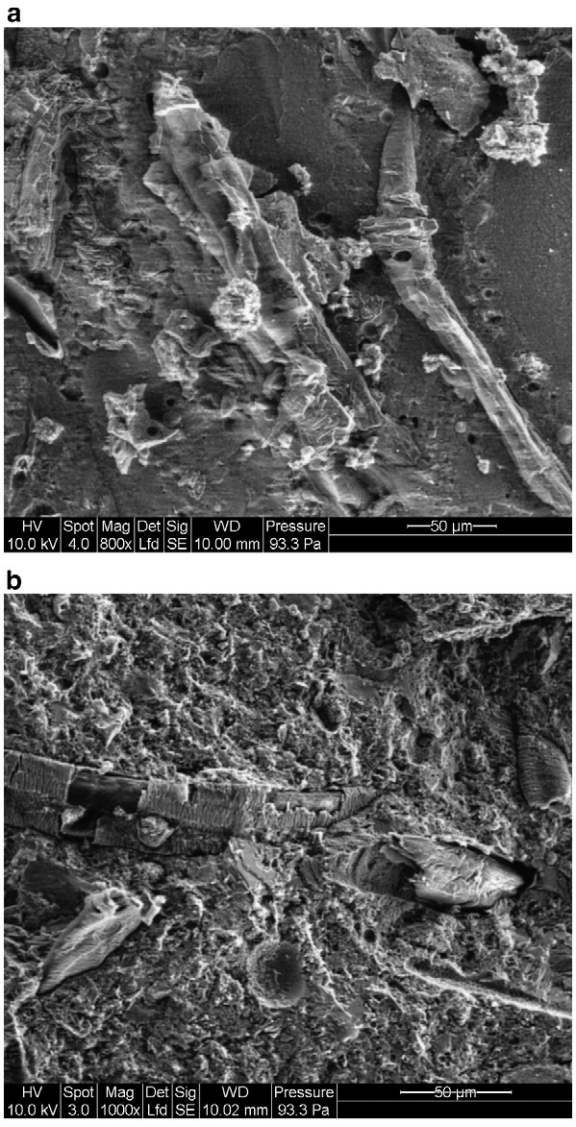

Fig. 7. ESEM micrographs of composite fracture surface after 25 wet/dry cycles. (a) Kraft pulp fiber-cement composite with 50% silica fume showing smooth homogenous matrix surface. (b) Kraft pulp fiber-cement composite with 10% silica fume showing typical matrix surface.

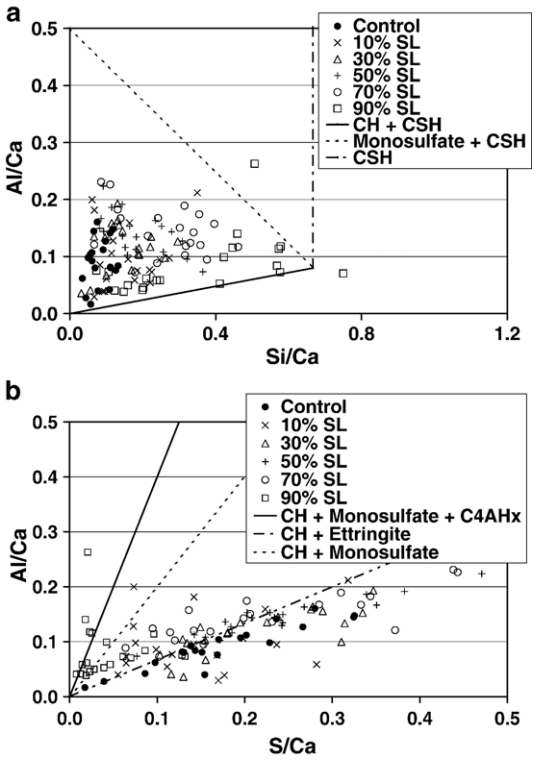

Fig. 8. Effect of slag on kraft fiber surface and cell wall chemical composition after 25 wet/dry cycles. (a) Average Al/Ca versus Si/Ca molar ratios. Note: the solid, short dashed, and long dashed lines represent the theoretical compositions of CH intermixed with C–S–H, monosulfate intermixed with C–S–H, and C–S–H, respectively. (b) Average Al/Ca versus S/Ca molar ratios. Note: the solid, short dashed, and long dashed lines represent the theoretical compositions of CH and C_4AH_x intermixed with monosulfate, CH intermixed with monosulfate, and CH intermixed with ettringite, respectively.

4.2. Calcium hydroxide content

The calcium hydroxide (CH) content of SCM-kraft pulp fiber cement composites prior to wet/dry cycling (i.e., 0 cycles) was determined by thermal analysis. Fig. 5 shows the trend between the CH content in the composite prior to cycling and post-cracking toughness after 25 cycles. When the CH content was greater than 2%, composite toughness after cycling was minimal. At CH contents less than 2%, toughness after cycling was considerably higher.

Thus, it is proposed that the initial CH content in the composite plays a significant role in minimizing degradation during wet/dry cycling. According to Mohr et al. [10], CH reprecipitation is a dominant step in kraft pulp fiber-cement composite degradation during wet/dry cycling. It is proposed that by minimizing the amount of calcium hydroxide initially present, by the use of SCMs, pulp fiber embrittlement due to CH reprecipitation is reduced or prevented.

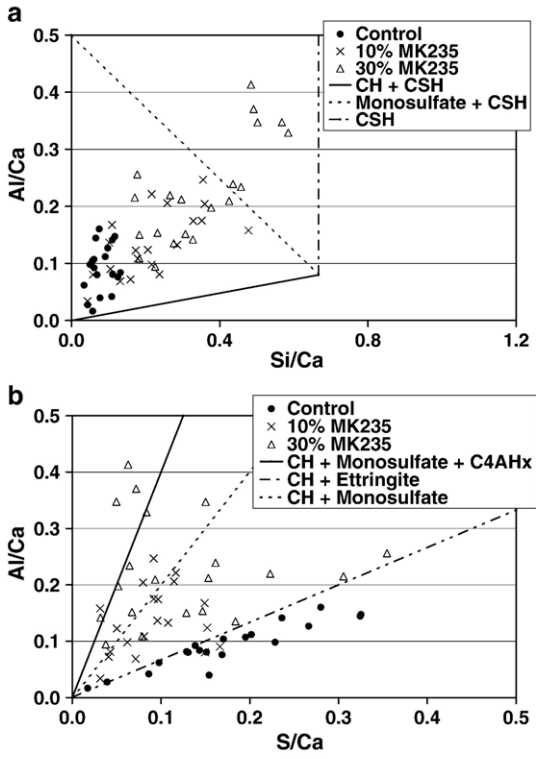

Fig. 9. Effect of metakaolin on kraft fiber surface and cell wall chemical composition after 25 wet/dry cycles. (a) Average Al/Ca versus Si/Ca molar ratios. Note: the solid, short dashed, and long dashed lines represent the theoretical compositions of CH intermixed with C–S–H, monosulfate intermixed with C–S–H, and C–S–H, respectively. (b) Average Al/Ca versus S/Ca molar ratios. Note: the solid, short dashed, and long dashed lines represent the theoretical compositions of CH and C_4AH_x intermixed with monosulfate, CH intermixed with monosulfate, and CH intermixed with ettringite, respectively.

4.3. Composite microstructure

In addition to examining the effects of SCMs on the alkali and calcium hydroxide contents, microstructural changes were investigated via ESEM. C–S–H, calcium hydroxide, monosulfate, and ettringite were identified in samples after 25 wet/dry cycles; results were comparable to those described in [10] where pulp fiber-cement composites, containing no SCMs, were similarly examined. It is generally accepted that the amount of calcium in the pore solution is decreased with SCM addition (as discussed in Section 4.2) by the formation of supplementary C–S–H. In addition, the formation of additional amounts of C–S–H may increase binding of trace sulfates and aluminates from the pore solution, decreasing their availability for reaction. This is similar to the increased alkali adsorption to C–S–H discussed in Section 4.1 [24].

As seen in Fig. 6, the partial replacement of portland cement with silica fume increased the relative amount of C–S–H present on the kraft fiber surfaces, as indicated by increasing Si/Ca with increasing silica fume replacement percentages. In addition, it is apparent that silica fume led to a decrease in the appearance of ettringite. It can be seen in Fig. 7a that the replacement of 30% or more of cement by weight with silica fume results in relatively smooth, homogenous matrix surface, primarily composed of C–S–H, as compared to a typical fracture surface appearance of a composite containing 10% silica fume (Fig. 7b).

Partial replacement of cement with slag also led to an increase in Si/Ca, compared to the control without SCMs, indicating the formation of supplementary C–S–H, but with little change in Al/Ca (Fig. 8a). Fig. 8b indicates that Al/Ca and S/Ca were not influenced by the use of slag, up to 90% replacement. With 90% slag, S/Ca notably decreases, indicating a change from sulfate-rich phases (e.g., ettringite) to alumina-rich phases (e.g., monosulfate and C_4AH_x). In Fig. 8a, a portion of the 90% slag composite data fell to the left of the theoretical monosulfate composition, indicating the presence of an Al-rich product on the fiber surfaces as the data fell along the theoretical composition line of monosulfate and calcium aluminate hydrate intermixed with calcium hydroxide. This suggests the formation of a calcium aluminate phase, perhaps C_4AH_x, on the fiber surface with 90% slag replacement.

Similar to the composites containing 90% slag, composites containing 30% metakaolin (MK235) showed significantly increased Al/Ca and Si/Ca (Fig. 9a), and decreased S/Ca (Fig. 9b) compared to the portland cement composites. Increasing metakaolin replacement percentages appeared to lead

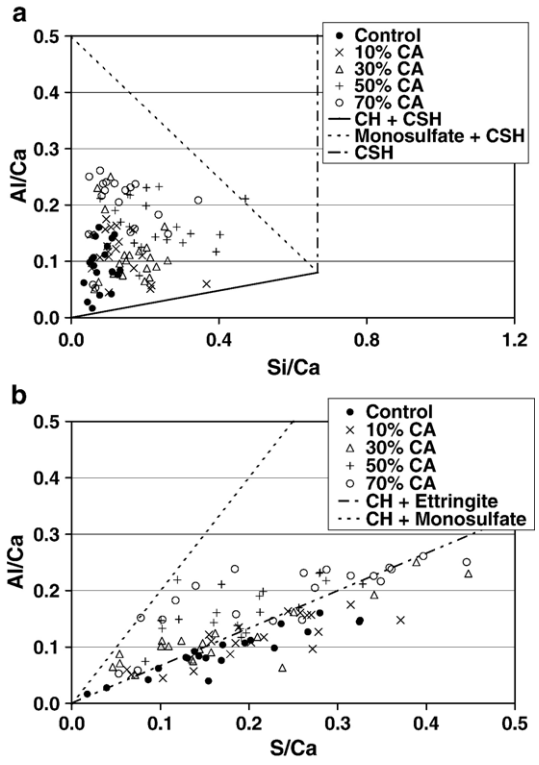

Fig. 10. Effect of Class C fly ash on kraft fiber surface and cell wall chemical composition after 25 wet/dry cycles. (a) Average Al/Ca versus Si/Ca molar ratios. Note: the solid, short dashed, and long dashed lines represent the theoretical compositions of CH intermixed with C–S–H, monosulfate intermixed with C–S–H, and C–S–H, respectively. (b) Average Al/Ca versus S/Ca molar ratios. Note: the short dashed and long dashed lines represent the theoretical compositions of CH intermixed with monosulfate and CH intermixed with ettringite, respectively.

to the formation of an Al-rich product; again, possibly C_4AH_x (Fig. 9b). Thus, although metakaolin is much more effective at lower replacement percentages, the mechanisms of improved durability for the slag and metakaolin samples seem to be similar and may be linked to the formation of a calcium aluminate product at the fiber surface. The consumption of calcium and aluminate ions from the pore solution is believed to decrease calcium hydroxide and secondary ettringite reprecipitation in the 90% slag and 30% MK235 composites (Figs. 8 and 9).

Class C fly ash, on the other hand, was not effective at improving composite durability. Fig. 10a shows that Si/Ca is only minimally increased with the use of fly ash, unlike the large increases observed with silica fume and metakaolin. In addition, Class C fly ash addition had a negligible effect on modifying the microstructure, as ettringite is predominant for all replacement amounts (Fig. 10b).

5. Discussion

Mechanical testing results for kraft pulp fiber-cement composites containing single, ternary, and quaternary SCM blends showed that the partial replacement of cement with SCMs can be effective in minimizing or even preventing composite degradation during 25 wet/dry cycles. Binary SCM composites that were most effective contained 30% SF, 50% SF, 90% SL, or 30% MK235.

Some ternary and quaternary SCM blends, chosen to optimize cost and performance, also minimized composite degradation during wet/dry cycling. These blends included 10% SF/70% SL, 10% MK235/70% SL, and 10% MK235/10% SF/70% SL. Thus, it can seen that combinations of the SCMs that performed well as binary blends with portland cement (i.e., silica fume, metakaolin, and slag), produced the ternary and quaternary blends of maximum efficiency. It is believed that these more practical SCM replacements of portland cement provided improvements in degradation resistance by the same mechanisms responsible in the higher percentage (i.e., less field practical) SCM composites. These mechanisms included a reduction in the amount of calcium hydroxide, an increase in ionic absorption from the pore solution with the formation of supplementary C–S–H, and subsequent reductions in ettringite reprecipitation (as discussed in Sections 4.1,4.2,4.3).

It was also observed that SCM fineness did not appear to influence composite degradation in these relatively small, cast-in-place composites. The metakaolins (MK235 and MK349) and diatomaceous earth/volcanic ash blends (DEVAcalcined and DEVAraw) varied in fineness, but mechanical testing (Tables 2–4) revealed that the finer SCMs (MK349 and DEVAraw) did not produce improved durability as compared to the coarser varieties (MK235 and DEVAcalcined). As discussed in Sections 3.4 and 3.5, the MK235 and MK349 particle fineness values were 11.1 m^2/g and 25.4 m^2/g, respectively. The DEVAcalcined and DEVAraw fineness values were 0.999 m^2/g and 2.654 m^2/g, respectively. Previous research [16] has shown that pore size refinement occurs by 28 days of age with the use of a higher surface area metakaolin. Thus, these results seem to indicate that a more refined composite pore structure did not improve the degradation resistance of these cast-in-place composites containing metakaolin or the DEVA blend. It may also be that a more refined pore structure led to an increased tendency for microcracking induced during wet/dry cycling. For example, the toughness of the 30% MK349 composite after 25 we/dry cycles was 1.57±0.22 MPa mm, compared to 7.32±1.11 MPa mm for the 30% MK235 composite. In addition, it has been shown that crystallization stresses due to CH and ettringite reprecipitation are greater in smaller pores [25]. This may also lead to increased microcracking in the MK349 and DEVAraw samples compared to those containing MK235 and DEVAcalcined.

To summarize, improvements in composite durability were observed by influencing two mechanisms of the prior degradation model [7,10]. Thus, as discussed in Sections 4.1–4.3, composite durability is most likely influenced by a particular SCMs' ability at a particular replacement level to reduce the calcium hydroxide content and to stabilize the alkali content. Therefore, the reprecipitation of ettringite is minimized through a reduction in Ca^{2+} due to the formation of supplementary C–S–H and/or Al-rich products, such as C_4AH_x. By reducing Ca^{2+} availability and alkali leaching, the tendency for secondary ettringite and calcium hydroxide reprecipitation diminishes, in favor of supplementary C–S–H, monosulfate, and C_4AH_x.

6. Conclusions

In this study, supplementary cementitious materials as a partial weight replacement for cement were investigated as a means to mitigate kraft pulp fiber-cement degradation during wet/dry cycling. Single, ternary, and quaternary blends of silica fume, slag, fly ash, metakaolin, and a diatomaceous earth/volcanic ash blend were used with ASTM Type I cement. Flexural testing was conducted after exposure to 0, 1, 2, 5, 10, 15, and 25 wet/dry cycles. Environmental scanning electron microscopy and thermal analysis were used to elucidate microstructural behavior and chemical changes. From mechanical testing and microstructural characterization, the following was observed:

- Composites containing 30% SF, 50% SF, 90% SL, and 30% MK235 apparently eliminated degradation due to wet/dry cycling, as measured by changes in strength and toughness with progressive cycling.
- Ternary and quaternary blends of 10% SF/70% SL, 10% MK235/70% SL, and 10% MK235/10% SF/70% SL also apparently prevented composite degradation, as measured by changes in strength and toughness, at more practical replacement values.
- In these small and relatively thin fiber-cement composites, a more reinforced pore structure do not seem to improve durability, as intuited from examinations of SCMs with similar composition but varying fineness.
- Improvements in SCM composite durability are most likely related to a reduction in the calcium hydroxide content and the stabilization of the alkali content. Thus, it is proposed

that ettringite and calcium hydroxide reprecipitation are minimized or prevented, leading to improved composite durability.

Acknowledgements

The authors would like to acknowledge the National Science Foundation (CMS-0556015, CMS-0122068, and DMR-0115961), the Institute of Paper Science and Technology (IPST)/Georgia Tech seed grant program, and IPST PATHWAYS program for their financial support. The authors also gratefully acknowledge the contributions of Dr. Hiroki Nanko, of MeadWestvaco, to this study.

References

[1] H. Gram, Methods for reducing the tendency towards embrittlement in sisal fibre concrete, Nord. Concr. Res. 2 (1983) 62–71.
[2] P. Soroushian, S. Marikunte, J. Won, Wood fiber reinforced cement composites under wetting–drying and freezing–thawing cycles, J. Mater. Civ. Eng. 6 (4) (1994) 595–611.
[3] S. Marikunte, P. Soroushian, Statistical evaluation of long-term durability characteristics of cellulose fiber reinforced cement composites, ACI Mater. J. 91 (6) (1994) 607–616.
[4] R.D. Tolêdo Filho, K. Scrivener, G.L. England, K. Ghavami, Durability of alkali-sensitive sisal and coconut fibres in cement mortar composites, Cem. Concr. Compos. 22 (6) (2000) 127–163.
[5] R.D. Tolêdo Filho, G.L. England, K. Ghavami, K. Scrivener, Development of vegetable fibre-mortar composites of improved durability, Cem. Concr. Compos. 25 (2003) 185–196.
[6] B.J. Mohr, H. Nanko, K.E. Kurtis, Durability of thermomechanical fiber-cement composites to wet/dry cycling, Cem. Concr. Res. 35 (8) (2005) 1646–1649.
[7] B.J. Mohr, H. Nanko, K.E. Kurtis, Durability of kraft pulp fiber-cement composites to wet/dry cycling, Cem. Concr. Compos. 27 (4) (2005) 435–448.
[8] S.A.S. Akers, J.B. Studinka, Ageing behavior of cellulose fibre cement composites in natural weathering and accelerated tests, Int. J. Cem. Compos. Lightweight Concr. 11 (2) (1989) 93–97.
[9] A. Bentur, S.A.S. Akers, The microstructure and ageing of cellulose fibre reinforced cement composites cured in a normal environment, Int. J. Cem. Compos. Lightweight Concr. 11 (2) (1989) 99–109.
[10] B.J. Mohr, J.J. Biernacki, K.E. Kurtis, Microstructural and chemical changes in pulp fiber-cement composites due to wet/dry cycling, Cem. Concr. Res. 36 (7) (2006) 1240–1251.
[11] Y.N. Ziraba, M.H. Baluch, A.K. Azad, Use of plasticized sulphur in sisal-fibre concrete, Durab. Build. Mater. 3 (1985) 65–76.
[12] B.J. Mohr, H. Nanko, K.E. Kurtis, Aligned kraft pulp fiber sheets for reinforcing mortar, Cem. Concr. Compos. 28 (2) (2006) 161–172.
[13] S.K. Canovas, N.H. Selva, G.M. Kawiche, New economical solutions for improvement of durability of portland cement mortars reinforced with sisal fibres, Mat. Struct. 25 (1992) 417–422.
[14] S.G. Bergstrom, H. Gram, Durability of alkali-sensitive fibres in concrete, Int. J. Cem. Compos. Lightweight Concr. 6 (2) (1984) 75–80.
[15] Justice J.M., Kennison L.H., Mohr B.J., Beckwith S., McCormick L., Wiggins B., Zhang Z.Z., Kurtis K.E. Comparison of two metakaolins and silica fume used as supplementary cementitious materials. In: Proceedings of the ACI 7th International Symposium on Utilization of High-Strength/ High Performance Concrete, SP-228, Detroit: American Concrete Institute, 2005: 213–235.
[16] Justice J.M., Kurtis K.E. Influence of metakaolin surface area on properties of cement-based materials. J ASCE Mat Civil Eng, in press.
[17] Kurtis K.E., Nanko H., El-Ashkar, N.H. US Patent 20020160174, 6 November 2001.
[18] El-Ashkar N.H., Nanko H., Kurtis K.E. Investigation of flexural properties of wood pulp microfiber cement-based composites. In: El-Dieb AS, Lissel SL, Reda Taha MM, editors. Proceedings of the International Conference on Performance of Construction Materials in the New Millennium. Cairo, Egypt, 2003. p. 1055–1064.
[19] ASTM C 348, Standard Test Method for Flexural Strength of Hydraulic-Cement Mortars, American Society for Testing and Materials, West Conshohocken Pennsylvania, USA, 2002.
[20] ASTM C 293, Standard Test Method for Flexural Strength of Concrete (Using Simple Beam With Center-point Loading), American Society for Testing and Materials, West Conshohocken Pennsylvania, USA, 2002.
[21] J.M. Richardson, J.J. Biernacki, P.E. Stutzmann, D.P. Bentz, Stoichiometry of slag hydration with calcium hydroxide, J. Am. Ceram. Soc. 85 (4) (2002) 947–953.
[22] H.F.W. Taylor, C. Famy, K.L. Scrivener, Delayed ettringite formation, Cem. Concr. Res. 31 (2001) 683–693.
[23] C. Famy, K.L. Scrivener, A. Atkinson, A.R. Brough, Influence of storage conditions on the dimensional changes of heat-cured mortars, Cem. Concr. Res. 31 (2001) 795–803.
[24] S. Mindess, J.F. Young, D. Darwin, 2nd Ed.Concrete: Prentice Hall, Upper Saddle River NJ, 2003.
[25] G.W. Scherer, Crystallization in pores, Cem. Concr. Res. 29 (1999) 1347–1358.